Strong-coupling cavity QED using rare-earth-metal-ion dopants in monolithic resonators: What you can do with a weak oscillator

D. L. McAuslan and J. J. Longdell*
Jack Dodd Centre for Photonics and Ultra-Cold Atoms, Department of Physics, University of Otago, Dunedin, New Zealand

M. J. Sellars
Laser Physics Centre, Research School of Physical Sciences and Engineering, Australian National University, Canberra, ACT 0200, Australia

(Received 13 August 2009; published 3 December 2009)

We investigate the possibility of achieving the strong coupling regime of cavity quantum electrodynamics using rare-earth-metal-ions as impurities in monolithic optical resonators. We conclude that due to the weak oscillator strengths of the rare-earth-metals, it may be possible but difficult to reach the regime where the single photon Rabi frequency is large compared to both the cavity and atom decay rates. However, reaching the regime where the saturation photon and atom numbers are less than one should be much more achievable. We show that in this "bad cavity" regime, transfer of quantum states and an optical phase shift conditional on the state of the atom is still possible and suggest a method for coherent detection of single dopants.

DOI: 10.1103/PhysRevA.80.062307 PACS number(s): 03.67.Lx, 82.53.Kp, 78.90.+t

I. INTRODUCTION

The interface between flying and stationary qubits is emerging as a key for progress in quantum information science. Impressive steps have been made toward quantum computing using both atomic [1–3] and photonic qubits [4,5]. The ability to reversibly transfer quantum states from single photons to single atoms would enable progress in both of these areas. From the point of view of optical quantum computing it would enable the single photon sources and memories they require [6]. From the point of view of quantum computing using atoms it provides a potentially scalable way of effecting qubit-qubit interactions [7,8].

The strong coupling regime of cavity quantum electrodynamics (cavity QED), that is the regime where an atom-cavity interaction in some way dominates the dissipation processes, is a necessity in order to enable the reversible transfer of states between atoms and photons. This regime is achieved by having an atom coupled to an electromagnetic field mode in a high-Q cavity. At present, strong coupling has been achieved experimentally using trapped atoms interacting with whispering gallery mode (WGM) [9,10], and Fabry-Pérot cavities [11–17]. It has also been observed in the solid state using quantum dots in WGM [18], micropillar [19], and photonic crystal cavities [20,21].

Rare-earth-metal-ion dopants are interesting systems to look at with respect to cavity QED. Like other solid state systems embedded in a dielectric they are particularly amenable to whispering gallery mode and microstructured resonators. The highest intensity for the mode functions of the resonances of such resonators are, in simple situations, inside the dielectric rather than outside. Compared to the difficulties of trapping atoms or ions in evanescent fields, the absolute position stability offered by state optical centers is also attractive.

Rare-earth-metal-ion dopants are at the same time much "cleaner" than other solid state systems that have been investigated. They have very long coherence times for their hyperfine transitions [22], among the longest of any qubit systems investigated. This would enable long term storage of photon states [23]. They do not suffer from the same spectral diffusion problems as quantum dots [24,25] and do not have the strong vibronic coupling of the nitrogen vacancy (NV) center [26].

Another reason for investigating cavity QED with rare-earth metals is that even if it is not possible to extend far into the strong coupling regime, the cavity is able to help with the detection of single dopant ions. Rare-earth-metal-ion dopants are particularity attractive systems for quantum computing. The long coherence times contrast strongly with large ion-ion interactions. These interactions are due to the fact that ions have static electric dipole moments and these dipole moments are different in the ground state and the excited state. The interaction strength for nearest neighbors is in the region of gigahertz [27]. Furthermore the large ratio of inhomogeneous to homogeneous broadening allows closely spaced ions to be easily addressed by tuning the exciting laser [28]. These properties have all been measured and rudimentary demonstrations using ensembles made [27–30]. While work has been done into improving the scalability using ensembles [31,32], and alternative architectures such as "read out ions" [32–34], the spin selective detection of a single rare-earth metal ion dopant would represent a significant step forward for rare-earth-metal-ion based quantum computing.

There are two important issues that need to be considered with regards to rare-earth-metal-ion and cavity QED. First the optical transitions have such long coherence times because their oscillator strengths are weak. This means that the atom-cavity coupling will be small, making it very difficult to achieve the "good cavity" strong coupling regime. Second the atomic decay rate can be several orders of magnitude larger than the spontaneous emission rate calculated only

*jevon@physics.otago.ac.nz

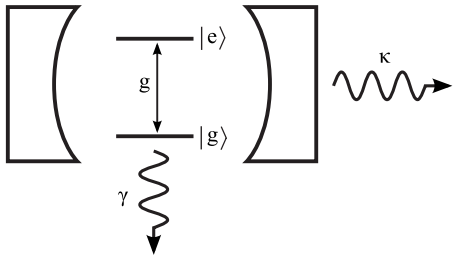

FIG. 1. Two-level atom in a cavity showing the three predominant interactions; g—the coupling between the atom and cavity, κ—the rate of decay out of the cavity, γ—the rate of decay through spontaneous emission of the atom.

from the oscillator strength of the transition to a certain level. This is due to spontaneous emission to a level other than the ground state followed by rapid nonradiative decay.

There have been a number of investigations into rare-earth-metal-ion dopants and optical cavities. Wang *et al.* [35] investigated a monolithic Fabry-Pérot resonator as a way of improving the efficiency of photon echoes used for classical signal processing. Ichimura and Goto [36] observed optical bistability and normal-mode splitting in a $Pr:Y_2SiO_5$ monolithic Fabry-Pérot resonator, and concluded that they were close to achieving the single atom strong coupling regime. Grudinin *et al.* [37] did calculations for Sm^{2+} ions in CaF_2 microcavities, and concluded that based on the properties of the free Sm^{2+} ion, the strong coupling regime should be possible. We are concerned with trivalent rare-earth-metal-ion which have superior coherence properties.

Here we discuss briefly the strong coupling regime for ideal weak oscillators and how this picture should change for the case of realistic decay processes. We survey a number of rare-earth-metal-ion doped systems and discuss their utility in strong coupling cavity QED experiments. We conclude by investigating some quantum information operations in the bad cavity regime. We show that the transfer of quantum states between atoms in distant cavities [7] is still possible and introduce a new method for calculating the driving fields needed for "quantum impedance matching." We also show that phase shifts on single photons conditional on the state of single atoms [38] is possible, and suggest a heterodyne based single atom detection scheme based on this.

II. MEANING OF STRONG COUPLING

We first consider a single two-level atom interacting with a single cavity mode and a continuum of other optical modes that will be treated as a bath. We will assume that the atom is sitting at an antinode of the cavity mode field. We will first examine the ideal case where the only relaxation process of the atom is due to its interaction with the optical fields. The dynamics of the system can be described by three rates: the coupling between a single atom and a single photon (g), the cavity decay rate (κ) and the atom spontaneous emission rate (γ). Figure 1 is a diagram of this model showing the interactions that occur.

From these constants one can derive two dimensionless numbers; the critical atom number (N_0), which describes the number of atoms required to have an appreciable effect on the cavity field, and the saturation photon number (n_0), the number of photons required to saturate an atom in the cavity. N_0 and n_0 are related to the system parameters by the following expressions:

$$N_0 \equiv \frac{\gamma\kappa}{g^2} \quad \text{and} \quad n_0 \equiv \frac{\gamma^2}{8g^2}. \tag{1}$$

We define the strong coupling regime as being when both the critical atom number and the saturation photon number are less than one, i.e., $(N_0, n_0) < 1$. By looking at Eq. (1) we can see that there are two ways that this condition can be achieved. The first is the "good cavity" regime, when the atom-field coupling is greater than the cavity and atomic decay rates i.e., $g > (\kappa, \gamma)$. Weak oscillator strengths make g small making it difficult to achieve $g > \kappa$. Fortunately weak oscillators also lead to small γ, and while g scales linearly with the transition dipole moment, the spontaneous emission rate scales as the transition dipole moment squared. So for weak oscillators one generally operates in the "bad cavity" regime, where the cavity decay rate is larger than the coupling strength, but hopefully the atomic decay rate is still small enough to make $N_0 < 1$.

For a single atom interacting with a single cavity mode we have the following interaction quantum Langevin equations [39,40]:

$$\dot{a} = g\sigma_- - \kappa a - \sqrt{2\kappa} b_{in}(t), \tag{2}$$

$$\dot{a}^\dagger = g\sigma_+ - \kappa a^\dagger - \sqrt{2\kappa} b_{in}^\dagger(t), \tag{3}$$

$$\dot{\sigma}_- = 2g\sigma_z a - \gamma\sigma_z\sigma_- + 2\sqrt{\gamma}\sigma_z d_{in}(t), \tag{4}$$

$$\dot{\sigma}_+ = 2ga^\dagger\sigma_z - \gamma\sigma_+\sigma_z + 2\sqrt{\gamma}\sigma_z d_{in}^\dagger(t), \tag{5}$$

$$\dot{\sigma}_z = -g(a^\dagger\sigma_- + \sigma_+ a) - \gamma\sigma_z - \frac{\gamma}{2} + \sqrt{\gamma}[\sigma_+ d_{in}(t) + \sigma_- d_{in}^\dagger(t)], \tag{6}$$

where $b_{in}(t)$ and $d_{in}(t)$ are the input fields associated with the cavity decay and spontaneous emission, respectively. Assuming that κ is much larger than the other time scales, we adiabatically eliminate the cavity mode by setting $\dot{a} = \dot{a}^\dagger = 0$,

$$a = \frac{g\sigma_- - \sqrt{2\kappa} b_{in}(t)}{\kappa}. \tag{7}$$

Substituting Eq. (7) into Eqs. (4) and (6) gives for σ_- and σ_z,

$$\dot{\sigma}_- = 2\left(\frac{g^2}{\kappa} + \frac{\gamma}{2}\right)\sigma_z\sigma_- - 2\sqrt{\frac{2g^2}{\kappa}}\sigma_z b_{in}(t) + 2\sqrt{\gamma}\sigma_z d_{in}(t) \tag{8}$$

$$\dot{\sigma}_z = -2\left(\frac{g^2}{\kappa} + \frac{\gamma}{2}\right)\sigma_z - \left(\frac{g^2}{\kappa} + \frac{\gamma}{2}\right) + \sqrt{\frac{2g^2}{\kappa}}[\sigma_+ b_{in}(t) + \sigma_- b_{in}^\dagger(t)] + \sqrt{\gamma}[\sigma_+ d_{in}(t) + \sigma_- d_{in}^\dagger(t)] \tag{9}$$

We can see that after adiabatically eliminating the cavity, the atoms are now described by two decay rates; $\frac{\gamma}{2}$ and $\frac{g^2}{\kappa}$. $\frac{\gamma}{2}$ represents the spontaneous emission of the atom into free space, and $\frac{g^2}{\kappa}$ represents the spontaneous emission of the atom through a cavity field mode. So in the regime where the critical atom number is small, $(N_0 \ll 1)$ the atom will decay through the cavity rather than into free space.

III. REALISTIC DECAY PROCESSES

For a perfect two-level atom the spontaneous emission rate can be calculated from the oscillator strength of the transition. In reality there are electronic levels present other than the two involved in the transition. The atom can spontaneously emit to one of these other levels, then relax the small energy gap to the ground state through much faster phonon decay processes [47]. This process can cause the atomic decay rate to be several orders of magnitude larger than the theoretical two-level spontaneous emission rate, as the decay rate now has to be calculated by summing the contributions from all of the allowed transitions. This decay from the excited state to other energy levels, followed by phonon decay does not have any effect on the dynamics of the atom except to cause the atomic decay rate (γ) to be larger. In particular the nuclear spin state of the atom is preserved because the decay is much more rapid than time scales over which the hyperfine interaction is appreciable. As a result the effect of this branched decay path does not change the ideal atom picture, except that the spontaneous emission rate γ may be disappointingly large if we expect it to be based only on the oscillator strength for the transition coupled to the cavity.

As well as the modification of γ because of decay to other energy levels, there is also broadening of the homogeneous linewidth (γ_h) due to excess dephasing. This dephasing, due to time dependent frequency shifts of the atoms, can be caused by processes such as excitation or relaxation of other ions, the nuclear and electron spins of the host material, and phonon scattering in the ion [41]. This last mechanism is temperature dependent and becomes negligible at cryogenic temperatures for the right material systems. In the case of cavity QED experiments the dominant cause of excess dephasing will most likely be interactions between spins in the host and the electron or nuclear spin of the dopant, as both the concentration of dopant and the amount of optical excitation in the sample will be small. Finding a good host for rare-earth-metal-ion dopants that does not contain nuclear spins has proved difficult, even in the quietest of hosts such as Y_2SiO_5, the nuclear spins of the yttrium contribute significantly to the homogeneous linewidths [41–43].

It has proved possible to "turn off" the excess dephasing due to nuclear spins in the hosts in hyperfine transitions in $Pr:Y_2SiO_5$ [22,44] by working at a specific field where the transition has zero first order Zeeman dependence. As well as hyperfine transitions, this technique should also be applicable to optical transitions in systems without electron spin, as long as the nuclear spin of the dopant is large enough $(>1/2)$ to provide a required anticrossing.

Here we will use γ for the population decay rate $(\gamma = 1/T_1)$. The homogeneous linewidth $\gamma_h = 1/T_2$ is the sum of linewidth due to population decay and excess dephasing (γ_p),

$$\gamma_h = \frac{\gamma}{2} + \gamma_p. \tag{10}$$

The treatment of the previous section can now be applied to the more realistic system that includes excess dephasing. We model the excess dephasing with an interaction Hamiltonian that couples the atom's population to the momentum of a bath of ground state harmonic oscillators,

$$H_{\text{int}} = i\hbar \sqrt{\frac{\gamma_p}{\pi}} \int \sigma_z [f^\dagger(\omega) - f(\omega)] d\omega \tag{11}$$

where the $f(\omega)$ are the bath operators. We then follow the approach of Gardiner and Collett [39,40].

We will again assume that we are in the regime where the cavity decays on a much faster time scale than dephasing of the dopant $(\kappa > \gamma_h)$. Again by adiabatically eliminating the cavity mode $(\dot{a} = \dot{a}^\dagger = 0)$ we derive the quantum Langevin equations,

$$\dot{\sigma}_- = 2\left(\frac{g^2}{\kappa} + \frac{\gamma}{2} + \gamma_p\right)\sigma_z\sigma_- - 2\sqrt{\frac{2g^2}{\kappa}}\sigma_z b_{in}(t) + 2\sqrt{\gamma}\sigma_z d_{in}(t) + \sqrt{2\gamma_p}\sigma_-[f_{in}^\dagger(t) - f_{in}(t)] \tag{12}$$

$$\dot{\sigma}_z = -2\left(\frac{g^2}{\kappa} + \frac{\gamma}{2}\right)\sigma_z - \left(\frac{g^2}{\kappa} + \frac{\gamma}{2}\right) + \sqrt{\frac{2g^2}{\kappa}}[\sigma_+ b_{in}(t) + \sigma_- b_{in}^\dagger(t)] + \sqrt{\gamma}[\sigma_+ d_{in}(t) + \sigma_- d_{in}^\dagger(t)], \tag{13}$$

where $f_{in}(t)$ is the input field associated with the bath operator $f(\omega)$. We can see that dephasing adds an extra term to the equation for $\dot{\sigma}_-$ which causes σ_- to now be described by the rates $\frac{g^2}{\kappa}$ and γ_h (instead of $\frac{\gamma}{2}$) which affects the coherence of the system. On the other hand $\dot{\sigma}_z$ is unchanged, which means that the population will still decay at the same rates as without excess dephasing.

So when dealing with cavity QED systems in the "bad cavity" limit and with excess dephasing, the system should be parametrized by two different critical atom numbers,

$$N_{0(pop)} = \frac{\gamma\kappa}{g^2}, \quad N_{0(ph)} = \frac{2\gamma_h\kappa}{g^2}, \tag{14}$$

where because $\gamma_h \geq \gamma/2$ the phase critical atom number is necessarily larger than the population critical atom number. A small value for the population critical atom number will ensure that if the dopant is excited the spontaneously emitted photon will predominantly be emitted from the cavity. If a single photon pulse in a single spatiotemporal mode or the coherent properties of the Fourier transform limited single photon pulse are required, or if one desires to probe the coherent properties of the atom-cavity system, then a small phase critical atom number is also necessary.

IV. OSCILLATORS STRENGTHS CAVITY PARAMETERS

We are interested in using WGM cavities for achieving strong coupling with rare-earth-metal-ions because they have

the ability to have small mode volumes (V) while at the same time having high quality factors (Q) [45,46]. We shall show that this ability to simultaneously have small V and high Q is required in order to achieve strong coupling in such a system.

Crystalline WGM resonators created using mechanical grinding and polishing techniques have achieved some of the highest quality factors of any small optical cavity, with Q factors up to 5.3×10^{10} being reported in CaF_2 resonators [37]. As coherent spectroscopy of rare-earth-metal-ion dopants is typically performed using doped crystals [47], crystalline WGM resonators are the logical choice for achieving strong coupling in such systems. Rare-earth metal doped glasses are another option for cavity QED experiments, as it is relatively simple to manufacture glass microsphere cavities with high quality factors (up to 8×10^9 in fused silica [48]). The problem with using doped glasses is that the homogeneous linewidth of the ions is several orders of magnitude larger than for crystalline hosts [47], which would make it very difficult to achieve strong coupling.

In order to reach the strong coupling regime we require the atom-cavity coupling to be large while the atomic and cavity decay rates are small. We here investigate how these rates specifically relate to rare-earth metal doped cavities, in particular WGM cavities. The cavity decay rate is given by [49]

$$\kappa = \frac{\pi c}{\lambda Q}, \tag{15}$$

where λ is the wavelength of light in the cavity. The coupling strength is given by the equation [36]

$$g = \frac{\mu}{n}\sqrt{\frac{\omega_a}{2\hbar\epsilon_0 V}}, \tag{16}$$

where n is the refractive index of the cavity and ω_a is the frequency of the transition. From this equation we can see that in order to have large coupling we require the cavity mode volume to be small. The transition dipole moment (μ) of the atom can be calculated from the atom's oscillator strength (f) using the expression [50]

$$\mu^2 = \frac{3\hbar e^2 n f}{2m_e\omega\chi_L}, \tag{17}$$

where $\chi_L=[(n^2+2)/3]^2$ is the local correction to the electric field to account for the fact that the ion is less polarizable than the bulk medium [50].

The transitions between $4f$ levels in the rare-earth metals are of particular interest when looking at cavity QED applications due to their long population and coherence lifetimes. Having long lifetimes means that the atomic decay rates are very small, which makes it easier to get into a strong coupling regime (because $\gamma\propto f$ and $g\propto\sqrt{f}$, as explained in Sec. II). Having small atomic decay rates makes it easy to get into a regime where $(\gamma,\gamma_h)<g$. This will enable the use of larger cavities than are traditionally used for cavity QED experiments, as $g\propto\frac{1}{\sqrt{V}}$. Using millimeter sized resonators is desirable for two main reasons: (1) they are easy to fabricate (can be made by hand using a standard lathe), (2) they can be tuned easily by deformation of the resonator. From Eq. (1) we can see that having a very small γ means that it is easy to achieve $n_0<1$. So when dealing with rare-earth metals the main issue is having κ small enough (high Q factor) that $N_0<1$.

The spontaneous emission time T_{spon} is the time it would take for the excited state of the atom to relax to the ground state if it was just a simple two-level atom with no other energy levels present. T_{spon} is related to the transition dipole moment of the atom [50]

$$T_{spon} = \frac{3\epsilon_0\hbar\lambda^3}{8\pi^2 n\chi_L\mu^2}. \tag{18}$$

In terms of the properties of the rare-earth-metal-ion transition (T_1,T_2,T_{spon}) we can write the critical atom and saturation photon numbers as

$$N_{0(pop)} = \frac{\gamma\kappa}{g^2} = \frac{\beta}{Q}\frac{T_{spon}}{T_1}\chi_L, \tag{19}$$

$$N_{0(ph)} = \frac{2\gamma_h\kappa}{g^2} = \frac{2\beta}{Q}\frac{T_{spon}}{T_2}\chi_L, \tag{20}$$

$$n_0 = \frac{\gamma\gamma_h}{4g^2} = \frac{\lambda\beta}{4\pi c}\frac{T_{spon}}{T_1T_2}\chi_L, \tag{21}$$

where we have introduced a new dimensionless parameter β that describes the mode volume of the cavity compared to the wavelength cubed [49],

$$\beta = \frac{8\pi^2 n^3 V}{3\lambda^3}. \tag{22}$$

Table I shows parameters for a number of rare-earth-metal-ion systems. Purely by looking at the ratios of $\frac{T_{spon}}{T_2}$ and $\frac{T_{spon}}{T_1}$ we would say that the $^3H_6$-$^3H_4$ transition in Tm^{3+}:$LiNbO_3$ would be the best option for investigating strong coupling, while the $^4I_{9/2}$-$^4F_{3/2}$ transition in Nd^{3+}:YVO_4 and the $^4I_{15/2}$-$^4I_{13/2}$ transition in Er^{3+}:Y_2SiO_5 are also possibilities. The $^3H_4$-$^1D_2$ transition in Pr^{3+}:YAG is another likely candidate as it has a small $\frac{T_{spon}}{T_1}$ ratio. The $\frac{T_{spon}}{T_2}$ ratio is not as good as the others, but by applying magnetic field to the system it should be possible to lengthen the dephasing time.

To see how the ion parameters relate to WGM cavities, in Fig. 2 we have plotted the cavity radius versus quality factor when $(N_{0(pop)},N_{0(ph)})=1$ for the different transitions using the fundamental TM mode $(n=1,m=\ell)$ of a spherical cavity. We can see that Er^{3+}:Y_2SiO_5 is clearly the best, although it does have the disadvantage of needing large magnetic fields to achieve good T_2 values. Nd^{3+}:YVO_4 and Tm^{3+}:$LiNbO_3$ also appear to be good candidates. These plots show that wavelength plays quite a large part in determining how suitable a transition is for strong coupling, which we would expect due to the $\frac{1}{\lambda^3}$ dependence of β.

V. THROW AND CATCH

One of the great promises of cavity QED is the ability to use light to transfer quantum states between the metastable

TABLE I. Parameters of rare-earth metal transitions. The magnetic field values next to each T_2 corresponds to the magnetic field used for the measurement.

Transition	λ (nm)	Oscillator Strength	μ (10^{-32} Cm)	T_{spon} (ms)	T_1 (μs)	T_2 (μs)	$\frac{T_{spon}}{T_1}$	$\frac{T_{spon}}{T_2}$
$^3H_4$-$^1D_2$ in Pr^{3+}:Y_2SiO_5	605.977 [51]	3×10^{-7} [41]	1.59	5.66	164 [41]	152 (77 G) [41]	34.5	37.2
$^3H_4$-$^1D_2$ in Pr^{3+}:YAG	609.587 [50]	1.5×10^{-6} [52]	3.53	1.11	230 [50]	20 (zero field) [50]	4.83	55.5
$^4I_{9/2}$-$^4F_{3/2}$ in Nd^{3+}:YVO_4	879.705 [50]	8×10^{-6} [50]	9.16	0.366	100 [53]	27 (15 kG) [41]	3.66	13.6
$^4I_{15/2}$-$^4I_{13/2}$ in Er^{3+}:Y_2SiO_5	1536.14 [50]	2×10^{-7} [54]	2.07	54.6	11400 [50]	4080 (70 kG) [50]	4.79	13.4
$^4I_{15/2}$-$^4I_{13/2}$ in Er^{3+}:$LiNbO_3$	1531.52 [50]	8×10^{-7} [54]	3.50	9.08	2000 [54]	80 (20 kG) [54]	4.54	113.5
$^3H_6$-$^3H_4$ in Tm^{3+}:$LiNbO_3$	794.264 [54]	5.044×10^{-6} [55]	6.37	0.382	170 [54]	32 (200 G) [54]	2.25	11.9
$^3H_6$-$^3H_4$ in Tm^{3+}:YAG	793.156 [50]	6.3×10^{-8} [50]	0.824	44.6	800 [50]	130 (100 G) [50]	55.8	343
$^7F_0$-$^5D_0$ in Eu^{3+}:Y_2SiO_5	579.879 [50]	1.3×10^{-8} [56]	0.324	120	1900 [50]	2600 (100 G) [50]	63.2	46.2

ground states of two different atoms [7]. Here we show this to be possible in the bad cavity regime and introduce a new method for calculating which pulse shape is required from the coupling beams in order to achieve the "quantum impedance matching."

Here we consider two lambda systems in two separate cavities with the output of one cavity driving the other as shown in Fig. 3.

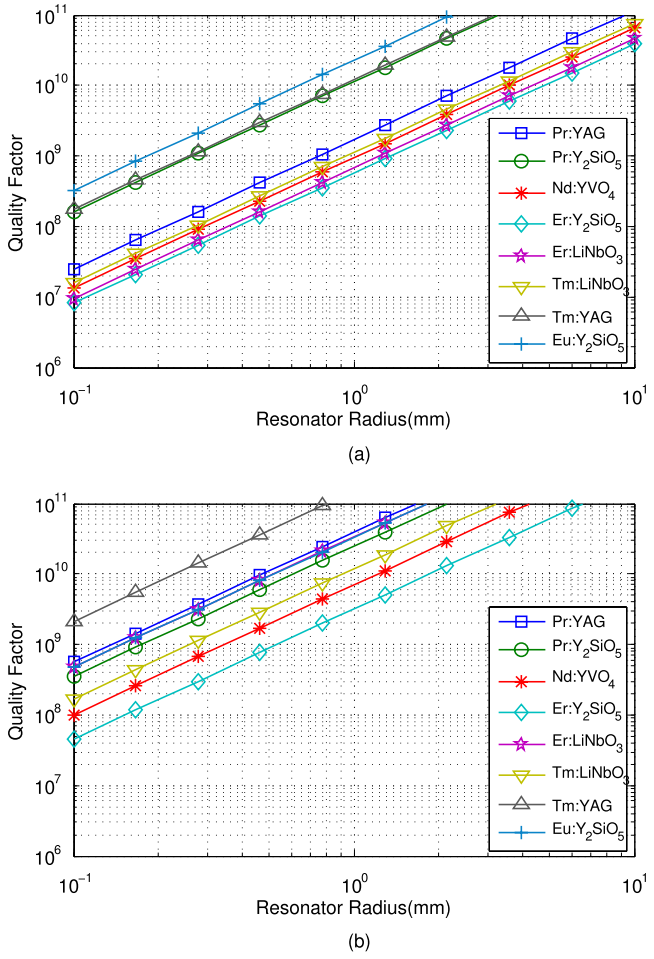

FIG. 2. (Color online) The resonator radius and quality factor required for (a) $N_{0(pop)}=1$, (b) $N_{0(ph)}=1$ for different rare-earth-metal-ions coupled to the fundamental mode in a WGM resonator.

We start with the Hamiltonian for a single Λ system in a cavity,

$$H = g(a^\dagger\sigma_{13} + a\sigma_{31}) + \Omega(t)(\sigma_{32} + \sigma_{23}). \tag{23}$$

Following a similar procedure to Sec. II we derive a set of Quantum Langevin equations that describe the time evolution,

$$\dot{\sigma}_{13} = -iga(\sigma_{11} - \sigma_{33}) - i\Omega(t)\sigma_{12}, \tag{24}$$

$$\dot{\sigma}_{12} = iga\sigma_{32} - i\Omega(t)\sigma_{13}, \tag{25}$$

$$\dot{a} = -ig\sigma_{13} - \kappa a - \sqrt{2}\kappa b_{in}(t), \tag{26}$$

where $\sigma_{13}=|1\rangle\langle 3|$, etc.

Because we are interested in the case of at most one excitation of this system, it is sufficient for us to consider the amplitudes given by

$$\phi_{12} = \langle \text{vac}, 1|\sigma_{12}|\psi\rangle, \tag{27}$$

$$\phi_{13} = \langle \text{vac}, 1|\sigma_{13}|\psi\rangle, \tag{28}$$

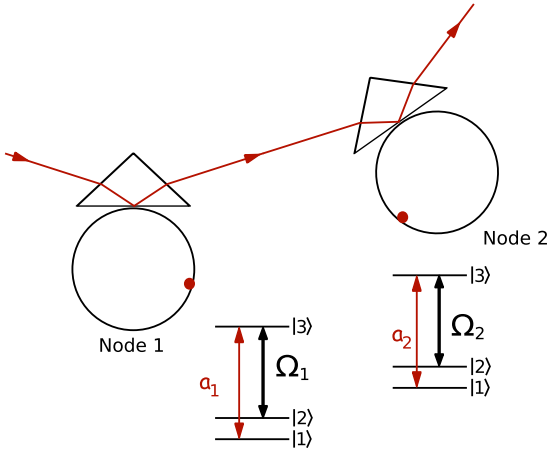

FIG. 3. (Color online) Throw and catch of photons between two atoms in separate cavities. The a_1 and a_2 represent cavity modes and Ω_1 and Ω_2 classical driving fields, perhaps introduced from the side of the cavity.

$$\alpha = \langle \mathrm{vac}, 1 | a | \psi \rangle, \tag{29}$$

where $\langle \mathrm{vac}, 1|$ refers to the cavity being in the vacuum state and the atom being in state 1. This leads to equations of motion,

$$\dot{\rho}_1 = \mathcal{L}_1 \rho_1, \tag{30}$$

where

$$\rho_1 = \begin{pmatrix} \alpha \\ \phi_{12} \\ \phi_{13} \end{pmatrix}, \quad \mathcal{L}_1 = \begin{pmatrix} -\kappa & 0 & -ig \\ 0 & 0 & -i\Omega_1(t) \\ -ig & -i\Omega_1(t) & 0 \end{pmatrix}. \tag{31}$$

Now suppose we arrange it so that the output of system 1 drives the input of system 2 (which is identical to system 1), i.e., $b_{in}=a_{out}$ then we can write a combined set of equations of motion for the entire system,

$$\frac{d}{dt}\begin{pmatrix} \rho_1 \\ \rho_2 \end{pmatrix} = \begin{pmatrix} \mathcal{L}_1 & 0 \\ X & \mathcal{L}_2 \end{pmatrix}\begin{pmatrix} \rho_1 \\ \rho_2 \end{pmatrix} \quad \text{where} \quad X = \begin{pmatrix} 2\kappa & 0 & 0 \\ 0 & 0 & 0 \\ 0 & 0 & 0 \end{pmatrix}. \tag{32}$$

Solving these equations will give an expression for $\Omega(t)$ showing how the Rabi frequency of the atoms needs to be driven in order to achieve a pulse being emitted at the first node which propagates and is then received at the second node (hence the throw and catch). To do this we write the equation of motion for the state vector ρ as

$$\dot{\rho} = A\rho + \Omega(t)B\rho + \sqrt{2\kappa}\begin{pmatrix} \beta_{in}(t) \\ 0 \\ 0 \end{pmatrix}, \tag{33}$$

where

$$A = \begin{pmatrix} -\kappa & 0 & -ig \\ 0 & 0 & 0 \\ -ig & 0 & 0 \end{pmatrix}, \quad B = \begin{pmatrix} 0 & 0 & 0 \\ 0 & 0 & -i \\ 0 & -i & 0 \end{pmatrix}. \tag{34}$$

We can take the input-output relation for the system:

$$\beta_{out} = \beta_{in} + \sqrt{2\kappa}[100]\rho \tag{35}$$

Differentiate twice with respect to t,

$$\dot{\beta}_{out} = \dot{\beta}_{in} + 2\kappa\beta_{in} + \sqrt{2\kappa}[100]A\rho, \tag{36}$$

$$\ddot{\beta}_{out} = \ddot{\beta}_{in} + 2\kappa\dot{\beta}_{in} + \sqrt{2\kappa}[100]A^2\rho + \sqrt{2\kappa}[100]AB\rho\Omega(t) + 2\kappa A(1,1)\beta_{in}. \tag{37}$$

This can then be rearranged to get an expression for the required Rabi driving field in terms of the input and output fields,

$$\Omega(t) = \frac{\ddot{\beta}_{out} - \ddot{\beta}_{in} - 2\kappa\dot{\beta}_{in} - 2\kappa A(1,1)\beta_{in} - \sqrt{2\kappa}[100]A^2\rho}{\sqrt{2\kappa}[100]AB\rho}. \tag{38}$$

Now we have an expression for the Rabi driving field that can be used to model the transfer of information between two nodes. This is done by setting the output field of the first node as a Gaussian and calculating the $\Omega(t)$ required to achieve this output. We then use the fact that absorbtion of a photon is the time reverse of emitting a photon to get the driving field at node 2, which is just the time reversed field at node 1. The results of a simulation showing successful quantum state transfer is shown in Fig. 4.

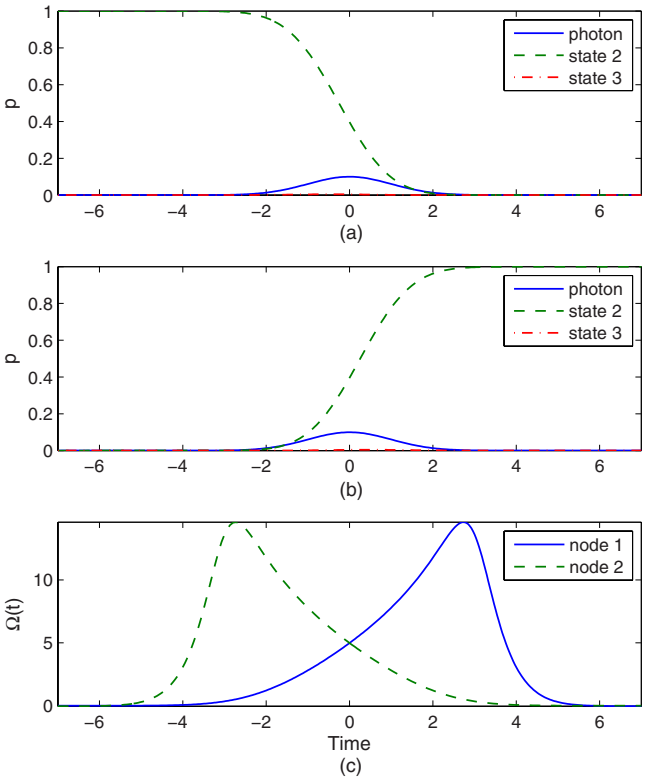

FIG. 4. (Color online) The results of simulation of quantum state transfer in the bad cavity regime. Graphs (a) and (b) show the atom and cavity populations for nodes 1 and 2, respectively. Graph (c) shows the classical driving fields applied to each node. The atom at node 1 starts off in state $|2\rangle$ and as the driving field is applied it gets transferred via a Ramen process to state $|1\rangle$, emitting a photon into the cavity mode in the process. This photon is then completely absorbed at node 2 placing that atom in state $|2\rangle$. Note that the units of time and $\Omega(t)$ are arbitrary and have been set to fit the parameters used in the simulation ($g=10$, $\kappa=2$, and $\gamma=0$).

VI. CONDITIONAL PHASE SHIFTS AND SINGLE DOPANT DETECTION

One way to use the optical cavity to enable single dopant detection is as a collecting lens for the fluorescence and then photon counting. This has a number of benefits over a conventional collecting lens: first the lens is narrow band meaning that it will only collect fluorescence over its linewidth, and second in the strong coupling regime the effective decay rate of the atom (g^2/κ) is increased leading to higher count rates. As in general the cavity will be resonant with the transition from one particular ground-state hyperfine level to one particular excited state hyperfine level, working in the strong coupling regime will improve the cyclicity of the transition.

This is important as except for complicated schemes based on parity conservation [57] it is difficult to find a cyclic transition in rare–earth-metal-ion dopants.

The emission rates will still be small, of the order of tens of kilohertz. This along with the poor cyclic nature of the rare-earth-metal-ion transitions, and finite dark count rates of single photon detectors, will make single state readout difficult.

Here we propose a single atom detection scheme based on coherent detection, inspired by the work of Wrigge *et al.* [58] and a quantum controlled phase-flip gate as described by Duan and Kimble [38].

Duan and Kimble proposed a quantum gate between a photon and the hyperfine state of an atom in a one-sided cavity. If the atom was in a state not involved in the transition coupled to the cavity mode, then the cavity was in effect empty and a single photon would be reflected from the cavity. If the atom was in a state involved in the transition coupled to the cavity mode, and if the system was in the good cavity strong coupling regime, then the effect of the atom was to split the cavity resonance in two and an incident photon would be reflected from the cavity with a π phase shift, much as it would be if the rear mirror of the cavity were not present.

Here we show that this conditional phase shift is still present in the bad cavity limit, even though the vacuum Rabi splitting is small compared to the cavity linewidth. This enables the presence of the atom to be detected as a narrow band phase shift on a weak coherent incident field.

To keep the phase shift as large as possible, we will assume that the input field is kept weak enough so as not to saturate the atom; in this situation the atom can be treated as a harmonic oscillator leading to quantum Langevin equations,

$$\begin{bmatrix} \dot{a} \\ \dot{s} \end{bmatrix} = \begin{bmatrix} -\kappa - i\delta & +g \\ -g & -\gamma/2 - i\delta \end{bmatrix} \begin{bmatrix} a \\ s \end{bmatrix} - \begin{bmatrix} \sqrt{2\kappa} & 0 \\ 0 & \sqrt{\gamma} \end{bmatrix} \begin{bmatrix} a_{in}(t) \\ s_{in}(t) \end{bmatrix}. \tag{39}$$

Here δ is the detuning between the input field and the cavity, a and s are the lowering operators for the cavity and atom, respectively. We shall assume the cavity is resonant with the dopant. We can calculate the spectral response of such a system if we assume the input field is narrow band compared to the dynamics of the atom-cavity system. Setting $\dot{a}(t)=\dot{s}(t)=0$ leads to

$$\begin{bmatrix} a \\ s \end{bmatrix} = \mathrm{Inv}\left(\begin{bmatrix} -\kappa - i\delta & +g \\ -g & -\gamma/2 - i\delta \end{bmatrix} \right) \begin{bmatrix} \sqrt{2\kappa} & 0 \\ 0 & \sqrt{\gamma} \end{bmatrix} \begin{bmatrix} a_{in}(t) \\ s_{in}(t) \end{bmatrix}, \tag{40}$$

which along with the input output relations gives

$$\begin{bmatrix} a_{out}(t) \\ s_{out}(t) \end{bmatrix} = \frac{1}{D} \begin{bmatrix} g^2 + (i\delta + \gamma/2)(i\delta - \kappa) & -\sqrt{2}g\sqrt{\kappa\gamma} \\ \sqrt{2}g\sqrt{\kappa\gamma} & g^2 + (i\delta - \gamma/2)(i\delta + \kappa) \end{bmatrix} \times \begin{bmatrix} a_{in}(t) \\ s_{in}(t) \end{bmatrix}, \tag{41}$$

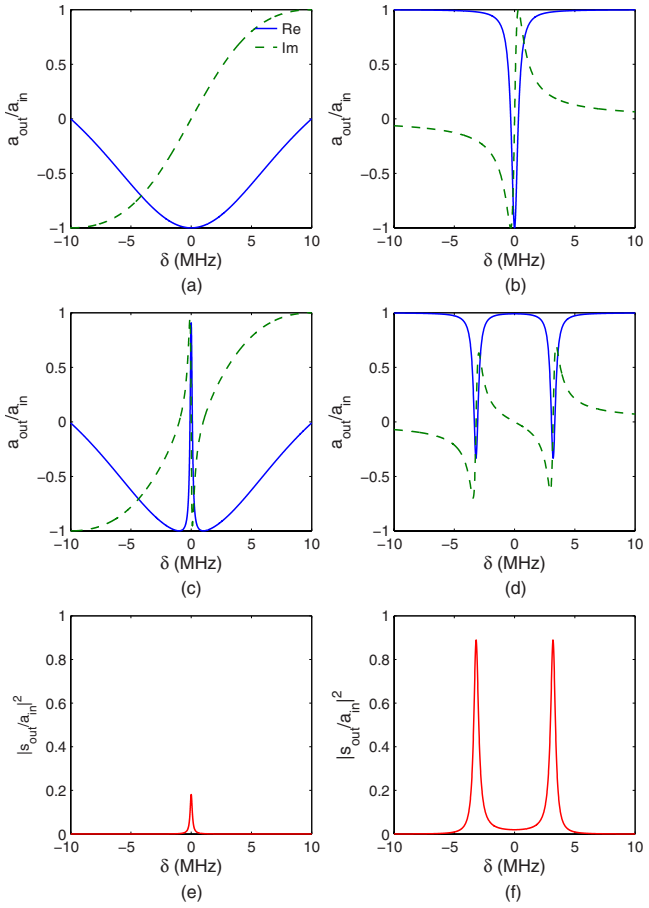

FIG. 5. (Color online) Phase of the cavity output as a function of detuning for [(a), (b)] an empty cavity; [(c), (d)] a cavity with an atom in it. Note that the cavity output at zero detuning undergoes a π phase shift when there is a resonant atom present. [(e), (f)] show the probability of the atom spontaneously emitting a photon vs detuning. The left plots correspond to an atom-cavity system in the bad cavity regime with parameters $(g,\kappa,\gamma)=(1,10,0.01)$ MHz. The right plots are for a system in the good cavity regime with parameters $(g,\kappa,\gamma)=(3.2,0.32,0.32)$ MHz.

where $D=g^2+(i\delta+\gamma/2)(i\delta+\kappa)$. Plots of this behavior is shown in Figs. 5 and 6.

Having an atom resonant in the cavity [Figs. 5(c) and 5(d)] causes a phase shift of π compared to the empty cavity case [Figs. 5(a) and 5(b)]. This shift occurs independent of whether we are in the good or bad cavity regime. Figures 5(e) and 5(f) show that in both regimes there is still a probability of the atom spontaneously emitting a photon, but the further we get into the strong coupling regime (i.e., the smaller N_0 is), the smaller this probability becomes, as shown in Fig. 6.

Coherent detection of the atom in this manner moves the problem from single photon counting with low count rates to the detection of narrow bandwidth phase shifts. In order to not be limited by the exciting laser its linewidth and drift should be small compared to the ions. State of the art stable lasers have both short and long term stability much greater than the kilohertz linewidths of rare-earth-metal-ions [59]. One benefit of the coherent approach is that the quantum efficiency of detectors used for homodyne and heterodyne

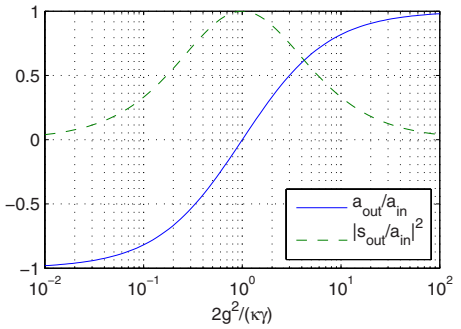

FIG. 6. (Color online) Phase shift and spontaneous emission probability vs $2g^2/\kappa\gamma$ for the case of zero detuning. For small values of g the atom is essentially uncoupled from the cavity, the input light is phase shifted by π. For $2g^2/\kappa\gamma=1$ there is no light output from the cavity and all the input light is lost as spontaneous emission. For large vales of g the incident light is phase shifted and the atom not excited, enabling the presence of the atom to be determined nondestructively.

detection is higher than photon counting detectors. The coherent approach will also be very insensitive to stray light, due to the spatial selectivity of the homodyne/heterodyne detection coupled with very small detection bandwidth. For these reasons the coherent approach should have both increased sensitivity and selectivity over photon counting.

In practice these narrowband phase shifts could be detected like an optical free induction decay. A brief, weak pulse exciting the atom-cavity system would lead to long-lived coherent emission at the same frequency as the ion. If this brief pulse was created as a phase modulated sideband from an electro-optic modulator with the carrier light off-resonance from the atom-cavity system, no interferometer would be needed, simplifying the implementation. In this way the approach could be considered as cavity-enhanced FM spectroscopy [60].

VII. CONCLUSION

We have investigated the use of rare-earth-metal-ions in cavity QED and determined that by using crystalline WGM cavities it should be possible to achieve the "bad cavity" strong coupling regime. We have showed that by operating in the bad cavity regime, quantum states can be reversibly transferred between atoms in separate cavities, which is an important requirement if we wish to use rare-earth metal doped cavities for quantum information processing. And finally we have devised a method of detecting single atoms by using an optical cavity and measuring the phase shift of photons that interact with this atom-cavity system.

[1] T. Pellizzari, S. A. Gardiner, J. I. Cirac, and P. Zoller, Phys. Rev. Lett. **75**, 3788 (1995).
[2] J. I. Cirac and P. Zoller, Phys. Rev. Lett. **74**, 4091 (1995).
[3] C. Monroe, D. M. Meekhof, B. E. King, W. M. Itano, and D. J. Wineland, Phys. Rev. Lett. **75**, 4714 (1995).
[4] Q. A. Turchette, C. J. Hood, W. Lange, H. Mabuchi, and H. J. Kimble, Phys. Rev. Lett. **75**, 4710 (1995).
[5] K. Mattle, H. Weinfurter, P. G. Kwiat, and A. Zeilinger, Phys. Rev. Lett. **76**, 4656 (1996).
[6] A. Kuhn, M. Hennrich, and G. Rempe, Phys. Rev. Lett. **89**, 067901 (2002).
[7] J. I. Cirac, P. Zoller, H. J. Kimble, and H. Mabuchi, Phys. Rev. Lett. **78**, 3221 (1997).
[8] H. J. Kimble, Nature (London) **453**, 1023 (2008).
[9] T. Aoki, B. Dayan, E. Wilcut, W. P. Bowen, A. S. Parkins, T. J. Kippenberg, K. J. Vahala, and H. J. Kimble, Nature (London) **443**, 671 (2006).
[10] B. Dayan, A. S. Parkins, T. Aoki, E. P. Ostby, K. J. Vahala, and H. J. Kimble, Science **319**, 1062 (2008).
[11] A. Boca, R. Miller, K. M. Birnbaum, A. D. Boozer, J. McKeever, and H. J. Kimble, Phys. Rev. Lett. **93**, 233603 (2004).
[12] A. D. Boozer, A. Boca, R. Miller, T. E. Northup, and H. J. Kimble, Phys. Rev. Lett. **97**, 083602 (2006).
[13] A. D. Boozer, A. Boca, R. Miller, T. E. Northup, and H. J. Kimble, Phys. Rev. Lett. **98**, 193601 (2007).
[14] Y. Colombe, T. Steinmetz, G. Dubois, F. Linke, D. Hunger, and J. Reichel, Nature (London) **450**, 272 (2007).
[15] J. McKeever, A. Boca, A. D. Boozer, J. R. Buck, and H. J. Kimble, Nature (London) **425**, 268 (2003).
[16] M. Trupke, J. Goldwin, B. Darquié, G. Dutier, S. Eriksson, J. Ashmore, and E. A. Hinds, Phys. Rev. Lett. **99**, 063601 (2007).
[17] T. Wilk, S. C. Webster, A. Kuhn, and G. Rempe, Science **317**, 488 (2007).
[18] K. Srinivasan and O. Painter, Nature (London) **450**, 862 (2007).
[19] J. P. Reithmaier, G. Sęk, A. Löffler, C. Hofmann, S. Kuhn, S. Reitzenstein, L. V. Keldysh, V. D. Kulakovskii, T. L. Reinecke, and A. Forchel, Nature (London) **432**, 197 (2004).
[20] K. Hennessy, A. Badolato, M. Winger, D. Gerace, M. Atatüre, S. Gulde, S. Fält, E. L. Hu, and A. Imamoğlu, Nature (London) **445**, 896 (2007).
[21] T. Yoshie, A. Scherer, J. Hendrickson, G. Khitrova, H. M. Gibbs, G. Rupper, C. Ell, O. B. Shchekin, and D. G. Deppe, Nature (London) **432**, 200 (2004).
[22] E. Fraval, M. J. Sellars, and J. J. Longdell, Phys. Rev. Lett. **92**, 077601 (2004).
[23] J. J. Longdell, E. Fraval, M. J. Sellars, and N. B. Manson, Phys. Rev. Lett. **95**, 063601 (2005).
[24] R. G. Neuhauser, K. T. Shimizu, W. K. Woo, S. A. Empedocles, and M. G. Bawendi, Phys. Rev. Lett. **85**, 3301 (2000).
[25] R. de Sousa and S. Das Sarma, Phys. Rev. B **68**, 115322 (2003).
[26] G. Davies and M. F. Hamer, Proc. R. Soc. London, Ser. A **348**, 285 (1976).
[27] N. N. Ohlsson, R. Krishna Mohan, and S. Kröll, Opt. Commun. **201**, 71 (2002).
[28] K. Ichimura, Opt. Commun. **196**, 119 (2001).
[29] G. J. Pryde, M. J. Sellars, and N. B. Manson, Phys. Rev. Lett. **84**, 1152 (2000).

[30] J. J. Longdell, M. J. Sellars, and N. B. Manson, Phys. Rev. Lett. **93**, 130503 (2004).
[31] I. Roos and K. Mølmer, Phys. Rev. A **69**, 022321 (2004).
[32] J. H. Wesenberg, K. Mølmer, L. Rippe, and S. Kröll, Phys. Rev. A **75**, 012304 (2007).
[33] M. Nilsson, L. Rippe, S. Kröll, R. Klieber, and D. Suter, Phys. Rev. B **70**, 214116 (2004).
[34] L. Rippe, M. Nilsson, S. Kröll, R. Klieber, and D. Suter, Phys. Rev. A **71**, 062328 (2005).
[35] T. Wang, C. Greiner, and T. W. Mossberg, Opt. Lett. **23**, 1736 (1998).
[36] K. Ichimura and H. Goto, Phys. Rev. A **74**, 033818 (2006).
[37] I. S. Grudinin, A. B. Matsko, A. A. Savchenkov, D. Strekalov, V. S. Ilchenko, and L. Maleki, Opt. Commun. **265**, 33 (2006).
[38] L. M. Duan and H. J. Kimble, Phys. Rev. Lett. **92**, 127902 (2004).
[39] C. W. Gardiner and M. J. Collett, Phys. Rev. A **31**, 3761 (1985).
[40] C. W. Gardiner and P. Zoller, *Quantum Noise*, 2nd ed. (Springer-Verlag, Berlin, Heidelberg, 2000).
[41] R. W. Equall, R. L. Cone, and R. M. Macfarlane, Phys. Rev. B **52**, 3963 (1995).
[42] R. W. Equall, Y. Sun, R. L. Cone, and R. M. Macfarlane, Phys. Rev. Lett. **72**, 2179 (1994).
[43] R. M. Macfarlane, T. L. Harris, Y. Sun, R. L. Cone, and R. W. Equall, Opt. Lett. **22**, 871 (1997).
[44] E. Fraval, M. J. Sellars, and J. J. Longdell, Phys. Rev. Lett. **95**, 030506 (2005).
[45] K. J. Vahala, Nature (London) **424**, 839 (2003).
[46] M. L. Gorodetsky, A. D. Pryamikov, and V. S. Ilchenko, J. Opt. Soc. Am. B **17**, 1051 (2000).
[47] *Spectroscopy of Solids Containing Rare Earth Ions*, edited by A. A. Kaplyanskii and R. M. Macfarlane (North-Holland Physics Publishing, Amsterdam, 1987).
[48] M. L. Gorodetsky, A. A. Savchenkov, and V. S. Ilchenko, Opt. Lett. **21**, 453 (1996).
[49] J. R. Buck and H. J. Kimble, Phys. Rev. A **67**, 033806 (2003).
[50] *Spectroscopic Properties of Rare Earths in Optical Materials*, edited by G. Liu and B. Jacquier (Tsinghua University Press and Springer-Verlag, Berlin, Heidelberg, 2005).
[51] G. Wang, Ph.D. thesis, Montana State University, 1997.
[52] Calculated.
[53] H. de Riedmatten, M. Afzelius, M. Staudt, C. Simon, and N. Gisin, Nature (London) **456**, 773 (2008).
[54] C. W. Thiel, Y. Sun, and R. L. Cone, (unpublished).
[55] X. Wang, Y. Ruan, T. Tsuboi, and V. V. Ter-Mikirtychev, in *Society of Photo-optical Instrumentation Engineers (SPIE) Conference Series*, edited by M. Eich, B. H. Chai, and M. Jiang (SPIE, Bellingham, WA, 1996), Vol. 2897, pp. 226–230.
[56] F. Könz, Y. Sun, C. W. Thiel, R. L. Cone, R. W. Equall, R. L. Hutcheson, and R. M. Macfarlane, Phys. Rev. B **68**, 085109 (2003).
[57] J. J. Longdell, Ph.D. thesis, The Australian National University, 2003.
[58] G. Wrigge, I. Gerhardt, J. Hwang, G. Zumofen, and V. Sandoghdar, Nat. Phys. **4**, 60 (2008).
[59] J. Alnis, A. Matveev, N. Kolachevsky, T. Udem, and T. W. Hänsch, Phys. Rev. A **77**, 053809 (2008).
[60] G. C. Bjorklund, Opt. Lett. **5**, 15 (1980).